J Mater Sci: Mater Med (2010) 21:2393–2401
DOI 10.1007/s10856-010-4088-3

Mg^{2+} substituted calcium phosphate nano particles synthesis for non viral gene delivery application

A. Hanifi · M. H. Fathi · H. Mir Mohammad Sadeghi · J. Varshosaz

Received: 5 February 2010 / Accepted: 26 April 2010 / Published online: 13 May 2010

Abstract Gene therapy provides a unique approach to medicine as it can be adapted towards the treatment of both inherited and acquired diseases. Recently, calcium phosphate vectors as a new generation of the non viral gene delivery nano carriers have been studied because of their biocompatibility and DNA condensation and gene transfer ability. Substituting cations, like magnesium, affects physical and chemical properties of calcium phosphate nano particles. In this study, Mg^{2+} substituted calcium phosphate nano particles have been prepared using the simple sol gel method. X-ray diffraction analysis, Fourier transform infra red spectroscopy, transmission electron microscopy, specific surface area analysis, zeta potential measurement and ion release evaluation were used for characterization of the samples. It was concluded that presence of Mg ions decrease particle size and crystallinity of the samples and increase positive surface charge as well as beta tricalcium phosphate fraction in chemical composition of calcium phosphate. These properties result in increasing the DNA condensation ability, specific surface area and dissolution rate of the samples which make them suitable particles for gene delivery application.

A. Hanifi (✉) · M. H. Fathi
Biomaterials Group, Materials Engineering Department, Isfahan University of Technology, 84156-83111 Isfahan, Iran
e-mail: a.hanifi@gmail.com

H. Mir Mohammad Sadeghi
Biotechnology Department, Faculty of Pharmacy and Pharmaceutical Sciences, Isfahan University of Medical Sciences, Isfahan, Iran

J. Varshosaz
Pharmaceutics Department, Faculty of Pharmacy and Pharmaceutical Sciences, Isfahan University of Medical Sciences, Isfahan, Iran

1 Introduction

Gene therapy provides a unique approach to medicine as it can be adapted towards the treatment of both inherited and acquired diseases [1]. There are two different approaches for gene delivery, viral and non viral. Non viral gene delivery systems have the potential to provide nucleic-acid-based therapeutics that closely resemble traditional pharmaceuticals [2].

Several major barriers need to be overcome for the development of non viral gene delivery systems for use in humans including; manufacturing, formulation and stability; extracellular barriers; and intracellular barriers [2, 3].

Non viral gene vector has to carry the gene to the surface of the target cell. As an extracellular barrier it has to overcome the immune system's protein interactions. Furthermore, the cellular association of naked DNA molecules is very poor, since negative charges on both the cell surface and the DNA molecules interrupt contact with each other via electrostatic interactions. A cationic vector enhances cell-surface binding through interactions with the negative constituents of the cell surface (e.g. heparan sulfate proteoglycans) or through selective binding to specific receptors, resulting in a strong transgene expression [1].

It is obvious that using cationic gene carriers has significant effect on negative charged DNA condensation and also cell surface bonding of the gene delivery system.

The DNA containing particles are subsequently taken up by cells via endocytosis, macropinocytosis, or phagocytosis in the form of intracellular vesicles [3]. Therefore, endosomal escape would be an important step in gene delivery process.

One promising strategy to release internalized complexes from the endosome is osmotic endosomal disruption or "proton sponge hypothesis" which is pointed out by

Boussif et al. [4]. In this mechanism, the carrier ionic release causes increasing the proton transfer into the endosome which makes the endosomal rupture and eventually gene will be released in the cytoplasm.

Several authors used inorganic nanoparticles for DNA delivery. Among them, calcium phosphate nanoparticles should be advantageous due to their high biocompatibility and good biodegradability [5].

In the case of calcium phosphate based approaches, lower levels of gene expression (in comparison to viral approaches) are observed because of difficulties associated with low concentration of nucleic acid condensed on calcium phosphate particles and endosomal escape of the DNA from endosome [6].

One way to address these concerns is to synthesize cationic calcium phosphate particles that possess both improved DNA condensing capabilities as well as higher DNA binding capacities. These characteristics would serve to increase the fraction of genetic material that successfully escapes the endosomal compartment which would thus lead to improved transfection efficiencies [6].

It has been demonstrated that calcium ions play an important role in endosomal escape, cytosolic stability and enhanced nuclear uptake of DNA through nuclear pore complexes. The special role of exogenous calcium ions to overcome obstacles in practical realization of this field suggests that calcium phosphate nanoparticles can be designated as second-generation non viral vectors for gene therapy [7].

Since degradation of beta tricalcium phosphate increases the amount of calcium ions inside the endosome and causes endosomal escape, producing cationic biphasic calcium phosphates composed of Hydroxyapatite (HA) and beta tricalcium phosphate (β-TCP) with nano size structure and optimized dissolution rate would be an applicable way to have an effective gene delivery system which is able to condense maximum amount of DNA, interact with cell membrane and receptors and also increase transfection efficiency. Substituting some cations and/or anions into the apatite structure can make such smart calcium phosphate carriers.

The calcium phosphate lattice easily incorporates a variety of substituent ions in the apatite structure, inducing modifications in powder cationic charge, crystallinity, particle morphology, lattice parameters and thermal stability [8, 9].

Substitution of cationic ions, such as magnesium ions, into the structure of calcium phosphates can increase the cationic charge of the calcium phosphate and inhibit crystal growth during the synthesis process [10].

Magnesium is closely associated with mineralization of calcified tissues, directly stimulating osteoblast proliferation [9, 11] and indirectly influences mineral metabolism [12]. Mg plays an essential role in the biological process due to its significant impact on the mineralization process and also its influence on HA crystal formation and growth [10].

The control of Mg^{2+} incorporation results in tailored crystallinity, solubility and morphology of the synthesized nanocrystals [8, 9]. Magnesium ions also have been found to inhibit growth of the (0 0 1) face of HA crystals [8, 13, 14].

It has been shown that the presence of Mg^{2+} within HA lattice sensibly affects apatite crystallization in solution and its thermal stability, promoting the formation of β-TCP [9]. Mg^{2+} can replace calcium (Ca^{2+}) ions in β-tricalcium phosphate ($Ca,Mg)_3(PO_4)_2$), causing structure stability [15, 16]. Mg substituted β-tricalcium phosphate is present in biologic systems and synthetic Mg substituted β-tricalcium phosphate has been proposed for osteoporosis therapy [15, 17] attaining acceptance for biomedical applications due to the extension of β-TCP stability caused by magnesium additions [15, 17].

Preparation of Mg substituted tricalcium phosphate has been reported by precipitation or hydrolysis methods in solution. These results indicate that the presence of Mg stabilizes the β-TCP structure. The incorporation of Mg also increases the transition temperature from β-TCP to α-TCP [18].

As reported by Schroeder et al. [19], β-TCP crystallizes in the rhombohedral space group, and the unit cell contains 21 cationic sites and 16 phosphate groups. Enderle et al. [20] examined β-TCP powders with Mg ranging from 0 to 20 mol% obtained by solid-state reaction using X-ray powder diffraction. A maximum 16 mol% of Mg^{2+} substitution on Ca(4) and Ca(5) sites in the β-TCP structure was found, corresponding to a solid solution with $(Ca_{0.86}Mg_{0.14})_3(PO_4)_2$ composition.

Dolci et al. mentioned the use of 0.5–200 nm HA powder containing up to 25.4wt% of Mg^{2+} for biomedical applications [21].

Mg substituted calcium phosphate powders have been prepared by precipitation and hydrolysis methods indicating limited replacement of Ca^{2+} with Mg^{2+} (up to 0.3 wt%) [22]. Some other studies on precipitation of Mg substituted calcium phosphate powders also showed substitution of Mg in HA [8]. Mayer et al. precipitated HA powders containing up to 1.5wt% of Mg without simultaneous carbonate substitution [23]. Golden and Ming managed to synthesize from aqueous solutions Mg substituted calcium phosphate powders with up to 2wt% of Mg [24]. Bigi et al. synthesized Mg substituted calcium phosphate powders with up to 5wt% of Mg in HA under hydrothermal conditions at 120°C [25]. Okazaki et al. substituted up to 5wt% of Mg in HA using precipitation method but with a total loss of crystallinity [26].

As a consequence of the aforementioned reports on preparing the Mg substituted calcium phosphate it has been

shown that having different amount of Mg concentration in apatite lattice results in changes in particle size, phase composition, dissolution rate and surface charge which can improve transfection efficiency of cationic calcium phosphate based non viral gene delivery systems.

Keeping this view of point the objective of this work is to synthesize magnesium substituted calcium phosphate nano particles using a simple wet chemical method aimed to study as a novel non viral inorganic gene delivery system. Having cationic charge and nano size structure will increase DNA condensation and concentration on the vector as well as endosomal escape through proton sponge mechanism.

2 Materials and methods

2.1 Sample preparation

Mg substituted calcium phosphate solution was prepared in the same process has been previously reported for pure HA [27]. Briefly, phosphoric pentoxide (P_2O_5, Aldrich), calcium nitrate tetrahydrate [$Ca(NO_3)_2{\cdot}4H_2O$, Aldrich] and magnesium chloride ($MgCl_2{\cdot}6H_2O$, Aldrich) were used to prepare precursors. A designated amount of Ca-precursor and P-precursor was mixed to form the Ca–P mixture. Mg-precursor was added drop-wise into Ca–P mixture to obtain a solution with (Ca, Mg)/P ratio of 1.67. Mg substituted calcium phosphate samples were prepared in four different concentration of Mg^{2+} ions in apatite lattice as it is described in Table 1.

The primary solution was stirred for 3 h at room temperature to form gel. The final gel was aged for 24 h at room temperature, washed, filtered, dried overnight at 80°C, and then calcinated in a Muffle furnace from room temperature to 600°C in the air. Calcination temperature and aging time has been chosen based on previous study [27, 28].

The atomic concentrations of elements (Ca, P and Mg) in the final samples were quantified by X-ray fluorescence spectroscopy (XRF) method (JEOL JSX-3201Z Element Analyzer) to compare that with as prepared concentration and stoichiometric ratio of Ca, P and Mg. Results are summarized in Table 1.

2.2 Phase composition, crystal size and crystallinity evaluation

Mg substituted calcium phosphate nano particles composition evaluated by X-ray diffraction (XRD, Philips X'Pert PRO, USA). The diffraction spectra were recorded in the 2θ range from 20° to 70° using Cu Ka (wavelength = 1.54056 Å, 40 mA, 40 kV) radiation with a step size of 0.05° and a step duration of 1 s.

Phase fraction of the products was measured using the method of Chung et al. [29]. Based on this method, the amount of HA in final product has an indirect relation with the I_{217} TCP/I_{211} HA ratio, where I_{217} TCP is the relation intensity of the (217) crystallographic planes of the TCP, and I_{211} HA is the relation intensity of the (211) crystallographic planes of the HA in the XRD patterns.

The crystal size of the samples was estimated from the XRD pattern using the Scherrer's equation [30]. According to this equation, a single-crystal dimension perpendicular to the (h k l) plane can be estimated from the peak broadening as:

$$D_{hkl} = k\lambda / B_{1/2}\cos\theta_{hkl} \quad (1)$$

where D_{hkl} (nm) is single crystal size, k is a constant varying with the method of measuring and is chosen to be 0.9, λ is the wavelength (nm) of Cu Kα radiation ($\lambda = 0.15418$ nm); $B_{1/2}$ corresponds to full width at half maximum (FWHM) for the peak hkl (rad) and θ_{hkl} is the diffraction angle (in degrees).

For samples with apatite structures, the line broadening of the (0 0 2) reflection was used to evaluate the crystal size, which corresponds to the c crystallographic axis.

According to Landi et al. [31] the crystallinity degree of samples (Xc) corresponding to the fraction of crystalline phase present in the examined volume was evaluated by the relation;

$$Xc \approx 1 - V_{112/300}/I_{300} \quad (2)$$

where I_{300} is the intensity of (3 0 0) reflection of HA and $V_{112/300}$ is the intensity of the hollow between (1 1 2) and (3 0 0) reflections, which completely disappears in non-crystalline samples. In agreement with Landi et al. a verification was done with the relation [9]:

Table 1 Mg substituted calcium phosphate samples composition with different Mg concentration

Sample name	Wt. % Mg		Ca/P ratio		(Ca + Mg)/P ratio		Calcination temp. (°C)
	As prepared	XRF	As prepared	XRF	As prepared	XRF	
0.00 Mg-CaP	0.00	0.05	1.67	1.70	1.67	1.71	600
0.25 Mg-CaP	0.25	0.23	1.62	1.63	1.67	1.66	600
0.50 Mg-CaP	0.50	0.59	1.56	1.54	1.67	1.61	600
1.00 Mg-CaP	1.00	1.07	1.5	1.48	1.67	1.59	600

$$Xc = \left(K/B_{1/2}\right)^3 \quad (3)$$

where K is a constant set at 0.24 and $B_{1/2}$ is the FWHM of the (0 0 2) reflection (in degrees).

2.3 Transmission electron microscopy evaluation

The particle size of the samples was examined by transmission electron microscopy (TEM, Philips CM30, USA). TEM samples were prepared using an ultrasound vibration method [32]. First, the samples were immersed in ethanol solution and subjected to ultrasound vibration for 15 min to disperse the precipitate powder homogeneously. Then, the precipitates were carefully extracted from the suspension of the sample and picked up using TEM copper meshes with carbon film coatings. After drying under ambient conditions, the samples on the copper meshes were examined by TEM.

2.4 FTIR spectroscopy

Characteristic functional groups were identified by Fourier transform infrared spectroscopy (FTIR, PerkinElmer, USA). The spectrum was recorded in the 4000–400 cm^{-1} region with 2 cm^{-1} resolution.

2.5 Specific surface area measurement

The specific surface area (SSA) of the nano particles was evaluated by the Brunauer–Emmett–Teller (BET) method using Micromeritics Device (Norcross, USA). The particle size (d_{BET}) was also estimated by assuming the primary particles to be spherical [9];

$$d_{BET} = 6/\rho \cdot s \quad (4)$$

where ρ is the theoretical density of the sample (3.156 g/cm^3 for pure HA and Mg substituted HA) and s is the specific surface area (SSA).

2.6 Measurement of nano particles surface charge

Since DNA has the net negative charge, cationic vectors with higher values of positive surface charge have better interaction with DNA and improve DNA condensation on the carrier [1, 3].

The surface charge of Mg substituted calcium phosphate nano particles was determined by measuring the zeta potential in the physiologic pH range. Zeta potential was measured with a Zetasizer Nano-ZS (Malvern Instruments Ltd., UK) and values were expressed as mean ± SD of three measurements.

2.7 Ca^{2+} Ions release measurement in simulated body fluid analysis

Since calcium ion release has a significant effect on endosomal escape of calcium phosphate gene delivery systems, simulated body fluid (SBF) was used to evaluate Ca^{2+} release form Mg substituted calcium phosphate nano particles.

Ion release test was performed in a stimulated body fluid medium of pH 7.4 at a ratio of 1 mg/ml in a water bath at 37°C. The SBF medium consists of 9 g NaCl, 5 g KCl and 0.2 g $MgHPO_4 \cdot 3H_2O$ per liter [33]. The dissolution of calcium ions in the SBF medium was determined by an atomic absorption spectrometer (AAS, PerkinElmer, USA).

3 Results and discussion

3.1 XRD phase analysis

XRD patterns of the Mg substituted calcium phosphate nano particles with different amount of Mg ions incorporated in apatite lattice are shown in Fig. 1.

With increasing Mg content, the XRD peaks became gradually broader. This effect could be explained by decreased crystallite size (Table 2) and increased lattice disorder associated with increasing Mg substitution in the calcium phosphate lattice.

Sample 1 (0.0 Mg-CaP) shows the characteristic peaks of HA which is in complete agreement with previous study [27, 33].

In the absence of Mg^{2+}, crystalline and stoichiometric HA was obtained, while in the presence of this ion,

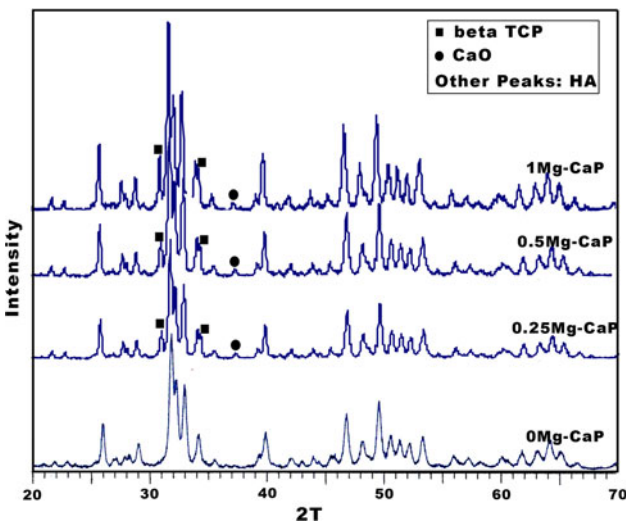

Fig. 1 XRD patterns of Mg substituted calcium phosphate nano particles with different amount of Mg concentration

Table 2 Single crystal size and crystallinity measured according to XRD patterns

Sample no.	Sample composition	Peak width (0 0 2) (rad)	Single crystal size (nm)	Crystallinity (Xc) (%)	HA/β-TCP (%)
1	0.00 Mg-CaP	0.0042	33.4 ± 3	64	97/3
2	0.25 Mg-CaP	0.0046	30.4 ± 2	59	91/9
3	0.50 Mg-CaP	0.0060	23.3 ± 1	53	82/18
4	1.00 Mg-CaP	0.0069	20.5 ± 1	51	74/16

biphasic calcium phosphate (BCP) could be synthesized composed of HA and β-TCP.

The shift of the XRD peaks with respect to the Mg free calcium phosphate (JCPDS card 09-0169) [34], serves as evidence of Mg substitution in prepared samples.

The HA phase observed in all samples probably contained some Mg^{2+} ions in the lattice as well.

In agreement with other studies, inducing the Mg ions in calcium phosphate structure stabilize the presence of β-TCP phase and result the biphasic calcium phosphate [8, 9, 12, 15, 19, 34–36]. Although there are some reports on preparing the Mg substituted calcium phosphate nano particles using acid–base reagents and high calcination temperature [37, 38], in this study using wet chemical simple sol gel method in an acid–base free solution and low calcination temperature, biphasic calcium phosphate with 0.25, 0.5 and 1.0 percent Mg substituted ions were synthesized.

Single crystal size, crystallinity and HA/β-TCP fraction of the samples are shown in Table 2. As it is reported in other studies [8, 10, 14], Increasing the amount of Mg substituted ions in apatite lattice inhibits the crystal growth and makes nano particles with smaller single crystal size.

Substitution of Mg^{2+} encourages the formation of β-TCP phase and reduces the crystallinity of the samples significantly. According to the data of Table 2, it is observed that Mg ions stabilize β-TCP phase and result in a biphasic calcium phosphate composed of HA and β-TCP phases in aqueous medium.

Since β-TCP dissolution rate in physiological environment is higher than HA, having these biphasic Mg substituted calcium phosphate nano particles with smaller crystal size and higher amount of β-TCP could improve the condensation of DNA on gene carrier as well as endosomal escape inside the cell using proton sponge mechanism as a result of higher concentration of Ca^{2+} which is presented in the solution from the samples with lower crystallinity values [4, 6, 7].

In addition, Table 2 shows that the Mg ions concentration more than 0.5% in calcium phosphate structure has more effect than lower concentration of Mg substituted ions on the physical and chemical properties of final products.

3.2 Transmission electron microscopy evaluation

The micrographs of Mg substituted calcium phosphate nano particles with 0.0, 0.25, 0.5 and 1.0% Mg ions that are shown in Fig. 2 show good agreements with the results of XRD measurements (Table 2).

All samples contain 20–35 nm particles and it could be observed that increasing the Mg value inhibits the particle growth and results in smaller nano particles.

Higher amount of Mg ions which are substituted for Ca ions in the structure has more effect on inhibiting the particle growth of the samples. TEM micrographs of the samples with different amount of Mg ions confirms the results of the XRD pattern evaluation and shows that the present simple wet chemical sol gel method can result in calcium phosphate nano particles which are applicable for gene delivery systems.

In this simple sol gel method, presence of magnesium ions helps to have smaller nano particles which their size is comparable with the result of other reports [8, 9, 12, 15, 19].

3.3 FTIR spectrum evaluation

FTIR spectra of the calcium phosphate nano particles with different amount of Mg^{2+} are shown in Fig. 3. These are typical spectra of HA showing PO_4^{3-} derived bands at 478, 566, 605, 963, and 1030–1090 cm^{-1} and adsorbed water bands at 1630 and 3000–3700 cm^{-1} [8, 39].

Loss of resolution of the PO_4^{3-} derived bands with increasing Mg content, were observed. This effect can be explained by decrease of crystallinity due to increased Mg substitution in the HA lattice [8].

Lower intensity of the OH^- derived bands could be caused by the increasing of adsorbed water because of the high surface area of the Mg substituted calcium phosphate at higher Mg content. This finding confirms the higher

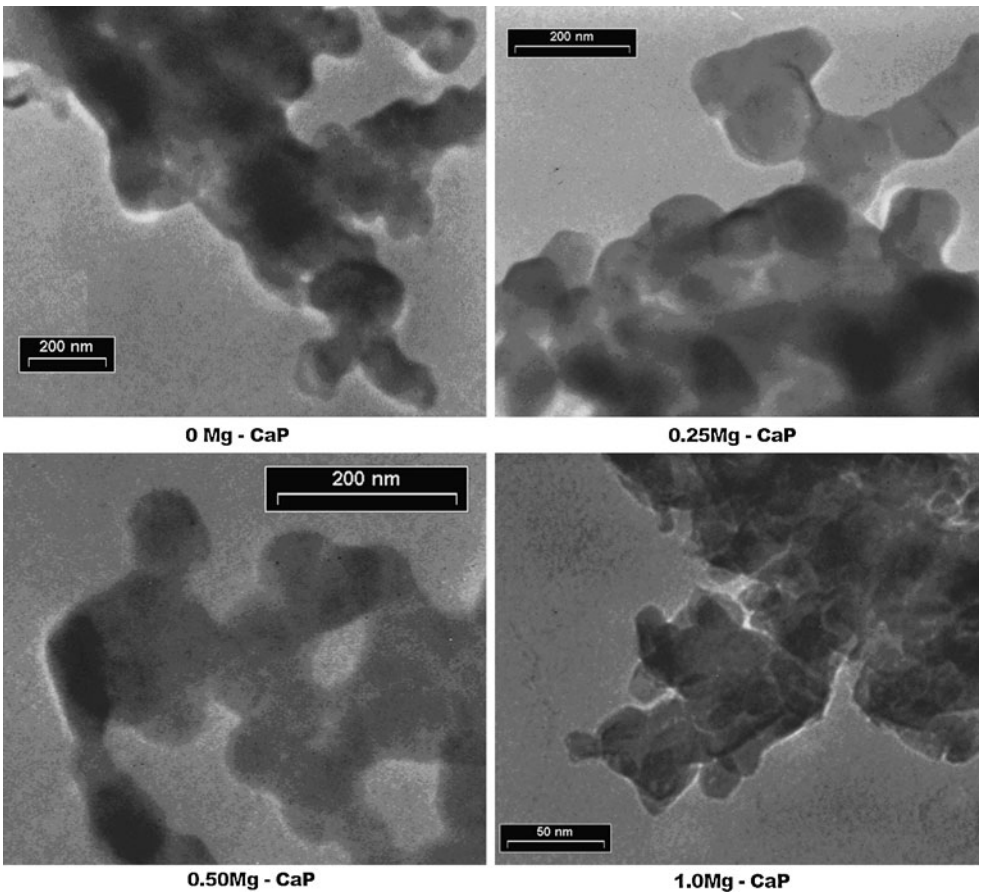

Fig. 2 TEM micrograph of Mg substituted calcium phosphate nano particles with 0.0, 0.25, 0.5 and 1.0% Mg ions

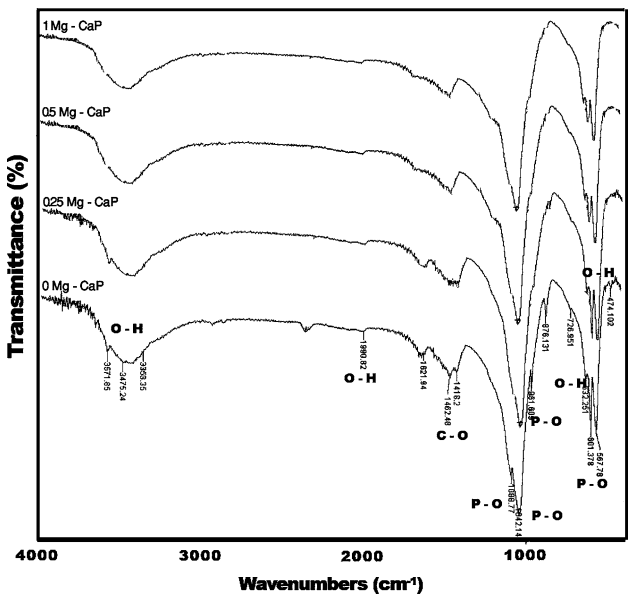

Fig. 3 FTIR spectrum of Mg substituted calcium phosphate nano particles

strength with which Mg-HA surface binds water molecules and consequently coordinates a higher number of water layers, compared to magnesium-free HA [40];

The presence of small amounts of CO_3^{2-} ions in all samples was due to presence of methanol as the solvent media and also calcination in air [33].

According to Riman et al. the position of the CO_3^{2-} derived bands indicates that CO_3^{2-}-for-PO_4^{3-} substitution dominates in the Mg substituted calcium phosphate but some fraction of the OH^- groups might be replaced by the CO_3^{2-} groups, which is usually observed in carbonated HA powders prepared by wet methods [8, 33].

3.4 Specific surface area

The specific surface area (SSA) values as well as the average particle sizes (d_{BET}) of all samples are presented in Table 3.

As it is expected sample 4 showed the highest SSA because of the highest amount of Mg ions in its structure.

Table 3 Specific surface area and d_{BET} of Mg substituted calcium samples

Sample no.	Sample composition	Specific surface area (m^2/g)	Equivalent spherical diameter d_{BET} (nm)
1	0.00 Mg-CaP	53	34
2	0.25 Mg-CaP	68	29
3	0.50 Mg-CaP	82	24
4	1.00 Mg-CaP	91	21

The calculated d_{BET} ranged between 21 and 34 nm. The results were in agreement with XRD measurement and TEM observation (Table 2 and Fig. 2).

It can be observed that in sample 2 and sample 3 the particle size decreased with Mg content, in good agreement with Zyman et al. [37]. But in the case of sample 4 (1 Mg-CaP), although in this study it shows the same behavior and keep decreasing the particle size with increasing the Mg content, Zyman et al. have reported that the sample with 1% Mg ions do not follow this trend. This contradiction could be because of the higher calcination temperature (1100°C) that they have used to calcinate their samples.

From Table 3 it can be concluded that by using 600°C calcination process, increasing the amount of Mg ions decreases the size of the resultant nano particles.

3.5 Nano particles surface charge

Table 4 shows the measured zeta potential value of all samples. Increasing the amount of the substituted ions in the structure makes nano particles with higher value of positive surface charge. It is in complete agreement with the previous studies [38] which reported positive surface charge for Mg substituted calcium phosphate nano particles.

Since the main mechanism of DNA binding to calcium phosphate nano particles is electrostatic interaction between cations (Ca^{2+}, Mg^{2+}) in calcium phosphate carrier and phosphate groups in DNA structure [41], increasing the net positive charge of the nano particles can improve DNA/vector interaction as well as DNA condensation. On the other hand a cationic vector enhances cell-surface binding through interactions with the negative constituents of the cell surface [1, 3]. Therefore Mg substituted calcium phosphate nano particles with higher values of positive surface charge could increase the transfection efficiency of the gene delivery system.

Table 4 Surface charge of Mg substituted calcium phosphate nano particles

Sample no.	Sample composition	Zeta potential (mV)
1	0.00 Mg-CaP	3.2 ± 0.5
2	0.25 Mg-CaP	6.7 ± 0.4
3	0.50 Mg-CaP	7.5 ± 1
4	1.00 Mg-CaP	8.0 ± 0.8

3.6 Calcium ion release regime

The calcium ions release of prepared calcium phosphate nano particles with different amount of Mg^{2+} into SBF medium is demonstrated in Fig. 4.

According to the data of Fig. 4, more calcium ions were released from the samples with higher Mg^{2+} values which is due to more degradation rate of these samples.

As it has been discussed above, having higher amount of magnesium ions in apatite lattice has several physical and chemical effects on the resultant nano particles, including; decreasing the crystal size, decreasing the crystallinity and increasing the stability of β-TCP (Tables 2 and 3). Therefore by increasing the amount of Mg ions, particles with a larger surface area are fabricated which contain a higher percentage of β-TCP phase. This causes an increase of dissolution rate of the nano particles. So, higher amount of Ca ions concentration could be observed for Mg contained samples in comparison with Mg free particles.

In agreement with the results of XRD pattern evaluation (Table 2), Mg concentration more than 0.5% has more effect on the Ca ion release of the samples. Higher release of Ca^{2+} has significant effect on endosomal escape of the gene delivery systems [7].

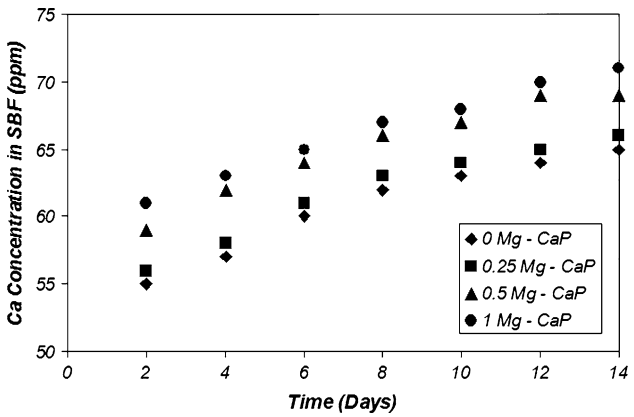

Fig. 4 Concentration of Ca^{2+} ions in SBF solution after predicted period of time

The results of this study show that substituting Mg ions in calcium phosphate structure can increase the release of calcium ions and potentially could increase the gene transfer efficiency. The study of gene delivery behavior of these novel calcium phosphate carriers would be the aim of the following work by the present authors.

4 Conclusion

Wet chemical synthesis of magnesium substituted calcium phosphate powders has been accomplished via a simple sol gel method. In present sol gel method, the ability to synthesize a stable form of biphasic calcium phosphate 20–35 nm particles composed of HA and β-TCP is largely dictated by the ability of Mg^{2+} ions to diffuse into the phosphate lattice enabling the transformation. Additionally, this would have a significant impact on the kinetics of the transformation reaction leading to the formation of a stable form of β-TCP.

The calcium phosphate powders without Mg^{2+} exhibited higher crystallinity and crystal size but lower amount of β-TCP in their composition. Substituting Mg ions in calcium phosphate structure make nano particles with smaller particle size, lower crystallinity, higher positive surface charge and higher amount of β-TCP which cause increasing in Ca ions release in simulated body fluid.

Particles with higher surface area (smaller crystal size) and positive surface charge would be able to condense more concentration of DNA on their surface that can increase the amount of DNA inside the cell and its nucleus. In addition, higher amount of β-TCP improves the gene delivery properties by increasing the dissolution rate of the carrier inside the endosome and causing endosomal rupture which release more concentration of DNA in cytoplasm and increase the gene delivery efficiency.

References

1. Taira K, Kataoka K, Niidome T. Non-viral gene therapy—gene design and delivery. Tokyo: Springer-Verlag; 2005.
2. Davis ME. Non-viral gene delivery systems. Curr Opin Biotechnol. 2002;13:128–31.
3. Gao X, Kim KS, Liu D, Nonviral gene delivery: what we know and what is next. AAPS J. 2007; 9(1):Article 9.
4. Boussif O, Lezoualc'h F, Zanta MA, Mergny MD, Scherman D, Demeneix B, Behr JP. A versatile vector for gene and oligonucleotide transfer into cells in culture and in vivo: polyethylenimine. Proc Natl Acad Sci USA. 1995;92:7297–301.
5. Sokolova V, Radtke I, Heumann R, Epple M. Effective transfection of cells with multi-shell calcium phosphate-DNA nanoparticles. Biomaterials. 2006;27:3147–53.
6. Olton D, Li J, Wilson ME, Rogers T, Close J, Huang L, Kumta PN, Sfeir C. Nanostructured calcium phosphates (NanoCaPs) for non-viral gene delivery: influence of the synthesis parameters on transfection efficiency. Biomaterials. 2007;28:1267–79.
7. Maitra A. Calcium phosphate nanoparticles: second-generation nonviral vectors in gene therapy. Expert Rev Mol Diagn. 2005;5(6): 893–905.
8. Suchanek LW, Byrappa K, Shuk P, Riman RE, Janas VF, TenHuisen KS. Preparation of magnesium-substituted hydroxyapatite powders by the mechanochemical–hydrothermal method. Biomaterials. 2004;25:4647–57.
9. Cacciotti I, Bianco A, Lombardi M, Montanaro L. Mg-substituted hydroxyapatite nanopowders: synthesis, thermal stability and sintering behaviour. J Eur Ceram Soc. 2009;29:2969–78.
10. Pina S, Olhero SM, Gheduzzi S, Miles AW, Ferreira JMF. Influence of setting liquid composition and liquid-to-powder ratio on properties of a Mg-substituted calcium phosphate cement. Acta Biomater. 2009;5:1233–40.
11. Lilley K, Gbureck U, Knowles J, Farrar D, Barralet J. Cement from magnesium substituted hydroxyapatite. J Mater Sci Mater Med. 2005;16:455–60.
12. Bracci B, Torricelli P, Panzavolta S, Boanini E, Giardino R, Bigi A. Effect of Mg^{2+}, Sr^{2+}, and Mn^{2+} on the chemico-physical and in vitro biological properties of calcium phosphate biomimetic coatings. J Inorg Biochem. 2009;103:1666–74.
13. Kannan S, Ferreira JMF. Synthesis and thermal stability of hydroxyapatite- beta-tricalcium phosphate composites with co-substituted sodium, magnesium, and fluorine. Chem Mater. 2006; 18:198–203.
14. Kanzaki N, Onuma K, Treboux G, Tsutsumi S, Ito A. Inhibitory effect of magnesium and zinc on crystallization kinetics of hydroxyapatite (0 0 0 1) face. J Phys Chem B. 2000;104:4189–94.
15. Arajo JC, Sader MS, Moreira EL, Moraes VCA, LeGeros RZ, Soares GA. Maximum substitution of magnesium for calcium sites in Mg-β-TCP structure determined by X-ray powder diffraction with the Rietveld refinement. Mater Chem Phys. 2009;118: 337–40.
16. Ito A, LeGeros RZ. Magnesium- and zinc-substituted beta-tricalcium phosphate materials. In: Vallet-Regi M, editor. Progress in bioceramics. Zurich: Trans Tech Publications; 2008. p. 85.
17. LeGeros RZ, Mijares D, Yao F, Tannous S, Catig G, Xi Q, Dias R, LeGeros JP. Synthetic bone mineral (SBM) for osteoporosis therapy: part 1—prevention of bone loss from mineral deficiency. Key Eng Mater. 2008;361–363:43–6.
18. Vecchio KS, Zhang X, Massie JB, Wang M, Kim CW. Conversion of sea urchin spines to Mg-substituted tricalcium phosphate for bone implants. Acta Biomater. 2007;3:785–93.
19. Schroeder LW, Dickens B, Brown WE. Crystallographic studies of the role of Mg as a stabilizing impurity in Ca_3 $(PO_4)2$ I. Refinement of Mg-containing β-Ca_3 $(PO_4)2$. J Solid State Chem. 1977;22:253–62.
20. Enderle R, Gotz-Neunhoeffer F, Gobbels M, Muller FA, Greil P. Influence of magnesium doping on the phase transformation temperature of β-TCP ceramics examined by refinement Rietveld. Biomaterials. 2005;26(17):3379–84.
21. Dolci G, Mongiorgi R, Prati C, Valdre G, Patent application no. WO 00/03747, 1998.
22. LeGeros RZ. Incorporation of magnesium in synthetic and in biological apatites. In: Fearnhead RW, Suga S, editors. Tooth enamel IV. Amsterdam: Elsevier; 1984. p. 32–6.
23. Mayer I, Schlam R, Featherstone JDB. Magnesium-containing carbonate apatites. J Inorg Biochem. 1997;66:1–6.
24. Golden DC, Ming DW. Nutrient-substituted hydroxyapatites: synthesis and characterization. Soil Sci Soc Am J. 1999;63: 657–64.
25. Bigi A, Falini G, Foresti E, Gazzano M, Ripamonti A, Roveri N. Magnesium influence on hydroxyapatite crystallization. J Inorg Biochem. 1993;49:69–78.

26. Okazaki M, Takahashi J, Kimura H. Comparison of crystallographic properties of Mg, Fe, Na, CO3, F, and Cl-containing apatites. J Osaka Univ Dent Sch. 1986;26:79–89.
27. Fathi MH, Hanifi A. Evaluation and characterization of nanostructure hydroxyapatite powder prepared by sol–gel method. J Mater Lett. 2007;61(18):3978–83.
28. Fathi MH, Hanifi A. Sol–gel derived nanostructure hydroxyapatite powder and coating: aging time optimization. Adv Appl Ceram. 2009;108(6):363–8.
29. Chung RJ, Hsieh MF, Huang KC, Chou FI, Perng LH. Preparation of porous HA/beta-TCP biphasicbioceramic using a molten salt process. Key Eng Mater. 2006;309–311:1075–8.
30. Patterson AL. The Scherrer formula for X-ray particle size determination. Phys Rev. 1939;56:978.
31. Landi E, Tampieri A, Celotti G, Sprio S. Densification behaviour and mechanisms of synthetic hydroxyapatites. J Eur Ceram Soc. 2000;20:2377–87.
32. Ren F, Xin R, Ge X, Leng Y. Characterization and structural analysis of zinc-substituted hydroxyapatites. Acta Biomater. 2009;5:3141–9.
33. Fathi MH, Hanifi A, Mortazavi V. Preparation and bioactivity evaluation of bone-like hydroxyapatite nanopowder. J Mater Process Technol. 2008;202:536–42.
34. Suchanek LW, Byrappa K, Shuk P, Riman RE, Janas VF, TenHuisen KS. Mechanochemical-hydrothermal synthesis of calcium phosphate powders with coupled magnesium and carbonate substitution. J Solid State Chem. 2004;177:793–9.
35. LeGeros RZ, Gatti AM, Kijkowska R, Mijares DQ, LeGeros JP. Magnesium tricalcium phosphate: formation and properties. Key Eng Mater. 2004;254–256:127–30.
36. Lee D, Sfeir C, Kumta PN. Novel in situ synthesis and characterization of nanostructured magnesium substituted β-tricalcium phosphate (β-TCMP). Mater Sci Eng C. 2009;29:69–77.
37. Zyman Z, Tkachenko M, Epple M, Polyakov M, Naboka M. Magnesium-substituted hydroxyapatite ceramics. Mat.-wiss. u. Werkstofftech. 2006;37(6):474–7.
38. Landi E, Tampieri A, Mattioli-Belmonte M, Celotti G, Sandri M, Gigante A, Fava P, Biagini G. Biomimetic Mg- and Mg, CO_3-substituted hydroxyapatites: synthesis characterization and in vitro behaviour. J Eur Ceram Soc. 2006;26:2593–601.
39. Elliott JC. Structure and chemistry of the apatites and other calcium orthophosphates. Amsterdam: Elsevier; 1994.
40. Sprio S, Tampieri A, Landi E, Sandri M, Martorana S, Celotti G, Logroscino G. Physico-chemical properties and solubility behaviour of multi-substituted hydroxyapatite powders containing silicon. Mater Sci Eng C. 2008;28:179–87.
41. W-Yih C, M-Shen L, Po-Hsun L, Pei-Shun T, Yung C, Shuichi Y. Studies of the interaction mechanism between single strand and double-strand DNA with hydroxyapatite by microcalorimetry and isotherm measurements. Colloids Surf A Physicochem Eng Asp. 2007;295(1–3):274–83.